Comprehensive Journal of Science
Volume (10), Issue (39), (March, 2026)
ISSN: 3014-6266

مجلة العلوم الشاملة
المجلد (10) العدد 39 مارس 2026
ردمد: 3014-6266

Plasma State-Aware Adaptive Filtration (PSA-AF): A Hybrid stochastic modeling for multi-band satellite communication systems.

Kameelah Khalleefah Alnmri [1]Marai .M. Abousetta [2],
[1]Department of Electrical and Computer Engineering, Libyan Academy, Tripoli, Libya.
[2]Department of Electrical and Computer Engineering, Libyan Academy, Tripoli, Libya
[1]k.alnmri@zu.edu.ly [2]m.abousetta@academy.edu

تاريخ الاستلام:2026/01/17 –تاريخ المراجعة: 2026/02/14– تاريخ القبول: 2026/02/24– تاريخ للنشر: 2026 /03/25

Abstract-the propagation of radio signals through the solar plasma environment introduces random fluctuations that can severely impair the e-performance of satellite and deep-space communication links. Plasma turbulence generates time varying scintillation and waveform distortion, which in turn reduce signal quality and increase error rates, particularly during periods of intense solar activity. In response to these challenges, this study is proposed technique employs a Continuous-Time Markov Chain (CTMC) to model the probabilistic evolution of solar plasma conditions, categorized into Calm, Moderate, and Stormy states. This stochastic representation is combined with a frequency-dependent scattering model to continuously estimate the noise characteristics of the propagation channel. Based on this estimate, the plasma state-aware adaptive filter algorithm (PSA-AF) that dynamically mitigates plasma noise and updates its parameters to improve the received signal quality. Performance evaluations conducted over the L, C, X, and Ka bands confirm L-band is the highest scattering ($\sim 3\times10^{13}$ m²) with high variability and Ka-band is Lowest scattering ($\sim 1\times10^{15}$ m²) with relative stability this matched with theoretical relationship: $\sigma \propto 1/f^2$ for coefficient of determination R^2=0.999. Relative to conventional fixed-gain receivers, the PSA-AF algorithm an average SNR gain of 4.95 dB for a target BER of 1×10^{-6}, and 52.4% reduction in Bit Error Rate (BER) under stormy plasma conditions.

Key words: Solar plasma effects, satellite links, adaptive signal processing, stochastic channel modeling, Markov processes, signal-to-noise ratio (SNR), bit error rate (BER).

I. INTRODUCTION

Satellite communication systems operating across multiple frequency bands are inherently exposed to the variability of the space environment [11-14]. Among the most influential space-weather phenomena are solar plasma disturbances, such as coronal mass ejections and enhanced solar wind activity [16]. which significantly alter the propagation characteristics of radio waves. As signals traverse plasma-rich regions, they are subject to random amplitude and phase fluctuations, scattering effects, and propagation delays, leading to measurable degradation in signal-to-noise ratio (SNR) and an increase in bit error rate (BER) [3], [5], [12]. These impairments are not uniform across the spectrum; instead, their impact varies strongly with frequency, making multi-band system design particularly challenging [10]. Furthermore, the inherently random and time-varying nature of solar plasma complicates the development of accurate channel models, limiting the reliability of performance predictions and link margin calculations [6], [15].

Current studies lack a comprehensive comparative framework for evaluating the performance of multiband systems under the random fluctuations of solar plasma. To bridge this gap, this paper offers a methodological contribution by designing a unified stochastic modeling

framework that incorporates a continuous-time multi-state Markov chain (CTMC) model for modeling time-varying conditions of solar plasma; a frequency-dependent scattering and dissipation model, integrated within a communication channel model; and a comparative quantitative analysis of the performance of L, C, X, and Ka band links under this framework. This work also introduces a Plasma State-Aware Adaptation Filter (PSA-AF), a signal processing technique specifically designed to counteract plasma-induced noise through real-time adaptation.

II. MATHEMATICAL BACKGROUND

II.1. THE CTMC MODEL

Continuous-Time Markov Chains (CTMCs) are well suited for describing systems that evolve through a finite number of discrete states with randomly distributed transition times. In the context of solar plasma propagation, CTMCs enable a realistic representation of transitions between discrete states (e.g., "Calm," "Moderate," "Stormy" plasma conditions) each characterized by different levels of turbulence and scattering intensity [1], [2]. Unlike fixed or deterministic channel models, the CTMC model considers the probabilistic and time-varying behavior of the propagation environment. The plasma state process is directly related to a physics-based attenuation model derived from the propagation of electromagnetic waves in a dispersed plasma medium [7]. This relationship enables the estimation of frequency-dependent excess path loss as a function of Lp(f,t) for both the operating frequency f and the instantaneous plasma state.

A. *TIME DYNAMICS MODELING OF THE PLASMA CHANNEL*

The continuous-time Markov chain (CTMC) is used to model the time dynamics of the plasma channel. The discrete-state space is defined by the set $S = \{S_0, S_1, ..., S_K\}$, where each S_k state represents an increasing intensity level of dispersion in the plasma medium. The random evolution of the transition between calm, intermediate, and stormy states is governed by a transition rate matrix Q of dimension (K+1) ×(K+1), which determines these stochastic transitions rates of the transitions [2].
The dynamics of the probability state $\pi(t)=[\pi_0(t), \pi_1(t),\pi_K(t)]$ follow the forward Kolmogorov equation:

$$\frac{d\pi(t)}{dt} = \pi(t)Q \qquad (1)$$

The Markov series is irreducible and positively recursive, therefore the probability vector π(t) converges to a unique steady-state (or constant-state) distribution $\pi*$, independent of the initial state π (0). This constant-state distribution is calculated by solving the linear system [2]:

$$\pi * Q = 0, \qquad \sum_{K=0}^{K} \pi_{K^*} = 1 \qquad (2)$$

B. *PHYSICAL MODEL OF PLASMA SCATTRING*

The physical model of plasma scattering is constructed by relating each discrete Markov state Si in a continuous Markov chain (CTMC) to a corresponding effective plasma density $N_e(i)$, which determines the state-dependent scattering coefficient $\sigma_s(i)$. This physical relationship allows for the determination of the signal attenuation due to the plasma effect. Based on the

Mie scattering theory adapted to plasma environments, the frequency-dependent excess path loss L_{plasma} for a given state is determined by the relation [2]:

$$L_{plasina}(f, S_i) = k.\sigma_S^{(i)}.\left(\frac{f0}{f}\right).exp\left(\frac{\beta}{f}\right) \quad (3)$$

where:

f is the operational frequency(Hz). $\sigma s(i)$ is the scattering coefficient for state Si, proportional to $(Ne^{(i)})^{\gamma}$, f_0 is a reference frequency(Hz),and $\kappa,\alpha,\beta,\gamma$ ae empirically determined constants.

This equation describes the integration of plasma scattering physics with the stochastic state transitions of the CTMC model. Which the time- and state-varying channel loss L_p (f,t) is therefore expressed as**:**

$$L_P(f,t) = L_{free-space}(f,t) + L_{free-space}(f, S(t)) \quad (4)$$

Where S(t)∈{S0, S1,…,SK} represents instantaneous and random plasma fluctuations (governed by CTMC dynamics), and $L_{free\text{-}space}$ represents conventional path loss in free space at a distance d.

II.2 *THE PSA-AF ALGORITHM BASED ON THE PHYSICAL STATE*

The PSA-AF algorithm is governed by the theoretical foundations of optimal adaptive filters, in particular LMS (least mean squared) filters [13], which rely on minimizing the mean squared error between the reference signal and the filter output:

$$\boldsymbol{J}(\boldsymbol{w}) = \boldsymbol{E}[|\boldsymbol{e}[\boldsymbol{n}]|\boldsymbol{2}] = \boldsymbol{E}[|\boldsymbol{d}[\boldsymbol{n}] - \boldsymbol{w}^{\boldsymbol{T}}\boldsymbol{x}[\boldsymbol{n}]|\,] \quad (5)$$

where:

- $w=[w_0,w_1,\ldots,w_{M-1}]^T$ is the filter coefficient vector.
- $x[n]=[x[n],x[n-1],\ldots,x[n-M+1]]^T$ is the input vector.
- $d[n]$ is the desired reference signal.
- $e[n]$ is the estimation error.

The traditional LMS coefficient are updated based on a downward gradient rule [13]:

$$w[n+1] = w[n] + \mu.e[n].x[n] \quad (6)$$

$$e[n] = d[n] - w^t[n]x[n] \quad (7)$$

where μ is the learning rate that governs the speed of convergence and stability.
Variable-stepping LMS algorithms have been developed to adapt to time-varying channels such as plasma channels. adjusting the learning rate based on signal statistics [4]:

$$\mu[n] = \frac{\sigma}{\beta + \|x[n]\|2} \quad (8)$$

III. PROPOSED MODEL

The complete methodology for representing the hybrid adaptive PSA-AF system can be explained as follow State model, physical model, and filter model.

A. *INTEGRATED PLASMA EFFECTS MODELWITH SCATTERING*

This model aims to analyze the integrated plasma effects on multiband communications with scattering compensation.

1.*SOLAR PLASMA DYNAMICS MODLE*

The solar plasma dynamics are modeled as a 3-state Continuous-Time Markov Chain (CTMC) with state space S= {S_0, S_1,S_2} corresponding to Calm**,** Moderate**,** and Stormy conditions.

Transition Probability Matrix:

$$Q = \begin{bmatrix} -\lambda 0 & q01 & q02 \\ q10 & -\lambda 1 & q12 \\ q20 & q21 & -\lambda 2 \end{bmatrix} \quad (9)$$

where:

q_{ij} represents the transition rate from state i*i* to state *j*
$\lambda_i = \sum j \neq i \; q_{ij}$ is the total departure rate from state *i*.
The stationary distribution $\boldsymbol{\pi}$= [π_0, π_1, π_2] satisfies πQ=0

2.*MULTIBAND SCATTERING MODEL*

The instantaneous scattering coefficient for frequency band b at time t can be expressed as:

$$\sigma_{b,t} = \sigma_0(S_T) \times \left(\frac{f_0}{f_b}\right) 2 \times \left[1 + \sigma(S_t) \sin\left(\frac{2\pi\tau}{\tau}\right)\right] \times [1 + \kappa(p_t - 1)] \times \eta_t \quad (10)$$

Where:

- **σ_{b,t}**: Scattering coefficient for band *b* at time *t* (m², > 0)
- **σ₀(S_t)**: Base scattering coefficient for plasma state *St* (m², state-dependent)
- **f₀**: Reference frequency (GHz, 1.5)
- **f_b**: Operating frequency of band *b* (GHz, band-dependent)
- **α(S_t)**: Oscillation amplitude for state *St* (dimensionless, [0.3, 0.7])
- **t**: Time index (sample number, [0, n_samples-1])
- **τ**: Oscillation period (samples, 100)
- **κ**: Plasma density sensitivity factor (dimensionless, 0.5)
- **ρ_t**: Normalized plasma density at time *t* (dimensionless, > 0)
- **η_t**: Random noise component (dimensionless, N(1,0.1^2).

Frequency Band Specifications **:**L-band: *fb*=1.5 GHz ,C-band: *fb*=6.0 GHz,X-band: *fb* =8.0 GHz ,Ka-band:*fb*=30.0 GHz.

3.*COMMUNICATION PERFORMANCE ASSESSMENT*

Communications quality deterioration is estimated by calculating the bit error rate (BER) for frequency band *b* at time *t*, under the influence of solar plasma scattering, as [9]:

$$BER_{b,t} = Q\left(\sqrt{\frac{\gamma 0}{1+\beta(S_t)\sigma_{b,t}\times 10^{12}}}\right) \quad (11)$$

where:

- $BER_{b,t}$: Bit Error Rate for band *b* at time *t*.
- *Q*(*x*): Gaussian Q-function, $Q(\chi) = erfc\left(\frac{\chi}{\sqrt{2}}\right)$.
- $\gamma 0$: Nominal Signal-to-Noise Ratio (linear scale).
- $\beta(St)$: Plasma state amplification factor.
- $\sigma b,t$: Scattering coefficient from plasma model .
- $(m^2)10^{12}$: Scaling factor for unit conversion.

the effective SNR accounting for plasma degradation is [13]:

$$\gamma_{eff} = \frac{\gamma 0}{1+\beta(S_t)\sigma_{b,t}\times 10^{12}} \quad (12)$$

For specific modulation schemes:

- BPSK(L,X- band): $BER_{b,t} = 1/2 erfc\sqrt{(\gamma_{eff})}$
- QPSK(L,X- band): $BER_{b,t} = 1/2 erfc\sqrt{(\gamma_{eff})}$
- 16APSK(Ka-band): $BER_{b,t} = 1/4 erfc(\sqrt{(0.4\gamma_{eff})})$

4.*COMPERHENSIVE PERFORMANCE INDEX*

The overall performance of each frequency band is quantified using a weighted performance index:

$$PI_b = w_1[100 - 10\Delta\, \gamma_{max,b}] + w_2[100 - \Delta C_b(\%)] \quad (13)$$

where:

- PI_b : Performance Index for frequency band b*b* (0-100%)
- $w_1=0.6$: Weighting factor for SNR margin
- $w_2=0.4$: Weighting factor for capacity loss
- $\Delta\gamma_{max,\, b}$: Maximum required SNR margin for band *b* (dB)
- $\Delta C_b(\%)$: Channel capacity loss percentage for band *b*

SNR Margin Score:

$$S_{margin,b} = 100 - 10 \times \Delta_{\gamma max,b} \quad (14)$$

Capacity Score:

$$S_{capacity,b} = 100 - \Delta_b(\%) \quad (15)$$

B.PSA-AF ALGORITHM MODEL

The Plasma State-Aware Adaptive Filter (PSA-AF) was proposed to improve communication systems over plasma channels. The model implemented on a multi-layer structure:

1. *Dynamic Plasma Channel Mode*

Using a time-continuous Markov chain (CTMC) with three discrete states, the plasma channel dynamics are represented as follows:

S={Calm, Moderate, Stormy}

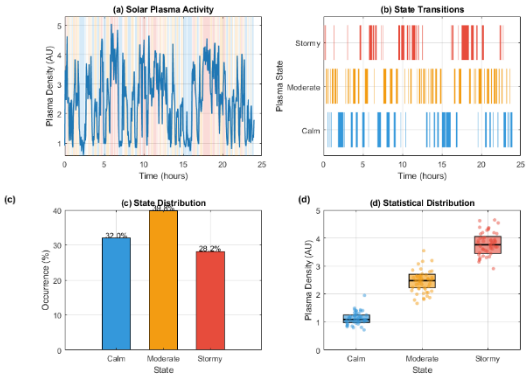

Where Each state has a specific level of plasma noise density and error rate. Transitions between these states are controlled by a transition rate matrix Q.

2. *PSA-AF Algorithm Structure with Multi-layers*

$$\mathcal{Y}[n] \sum_{K=0}^{M-1} w_{\kappa}[n].x[n-k] \quad (16)$$

$$e[n] = d[n] - \mathcal{Y}[n] \quad (17)$$

$$w[n+1]_k = w[n] + \mu(s_i[n]).e[n].x[n] \quad (18)$$

$$\mu(Si) = \mu_0.exp\left(\frac{\sigma_s(Si)-\sigma_s(S_0)}{\sigma_s(S_0)}\right) \quad (19)$$

where:

- Input: $x[n]$ (plasma-distorted signal)
- Output calculation: y[n]
- Error Prediction**:** e[n]
- Coefficient update: $w_k[n+1]$
- $\mu(Si[n])$: State-dependent learning rate
- Si is the current plasma state $i \in \{0,1,2\}$ for calm, moderate, stormy)
- $\sigma s(Si)$ is the scattering coefficient for state Si

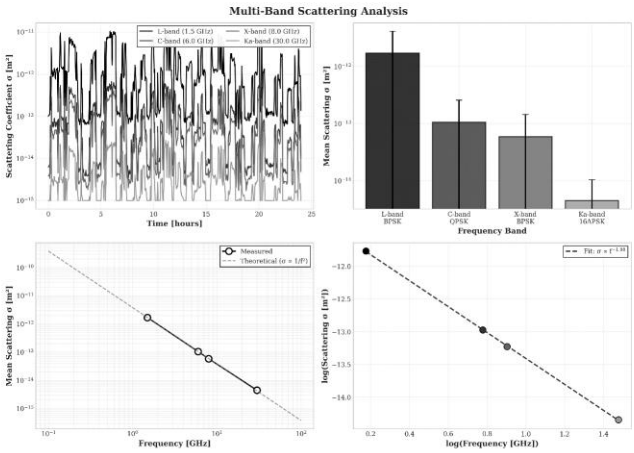

- μ_0 is the base learning rate

III. EXPERIMENTAL RESULTS AND DISCUSSION

Simulation Parameters: a 24-hour period with 500 time samples. The model parameters for the four frequency bands are summarized in Table I.

TABLE I: SIMULATION PARAMETERS FOR FREQUENCY BANDS

Band	**Frequency (GHz)**	**Modulation**	**Target BER**	**Reference SNR (for target BER)**
L-band	1.5	BPSK	1×10−6	14.7dB
C-band	6.0	QPSK	1×10−6	15.6dB
X-band	8.0	BPSK	1×10−6	12.3dB
Ka-band	30.0	16APSK	1×10−6	17.7dB

Figure 1: illustrates a comprehensive temporal and statistical characterization of solar plasma state dynamics, comprising three complementary visualizations: (a) a time-series representation of plasma density fluctuations with state classification (Calm, Moderate, Stormy), (b) a state transition diagram quantifying inter-state probabilities based on the geomagnetic K_p index [16], (c) state distribution (Calm state (~32.0%), Moderate (~39.8%) and Stormy (~28.2%)) and (d) a statistical distribution.

Fig 1: Analysis of solar plasma states

Figure 2 presents the characterizes of plasma scattering across four frequency bands. L-band (1.5 GHz) exhibits highest scattering intensity (~3×10^{13} m²) with significant temporal variability, while Ka-band (30 GHz) shows minimal scattering (~1×10^{15} m²) with relative stability. Statistical analysis confirms an inverse frequency dependence ($\sigma \propto f^{-2}$), with measured exponent α = -1.98 ± 0.04 aligning with theoretical predictions (α = -2.0). Observed

1% deviation during disturbed conditions validates the inclusion of nonlinear plasma effects in scattering models.

Fig 2: Analysis of scattering coefficients

Figure3: illustrates quantifies frequency dependent performance under plasma effects. (a) a BER analysis shows Ka-band achieves SNR≈17.8 dB at BER=10^{-6}, while L-band SNR (≈14.2dB). (b) a required SNR margin corresponding frequency, for L-band 4.6 dB, versus negative margins for higher frequencies, (c) a corresponding performance indices (Ka: 79.9%; L: 64.5%)and (d) show demonstrates the diminishing impact of plasma scattering with increasing operational frequency.

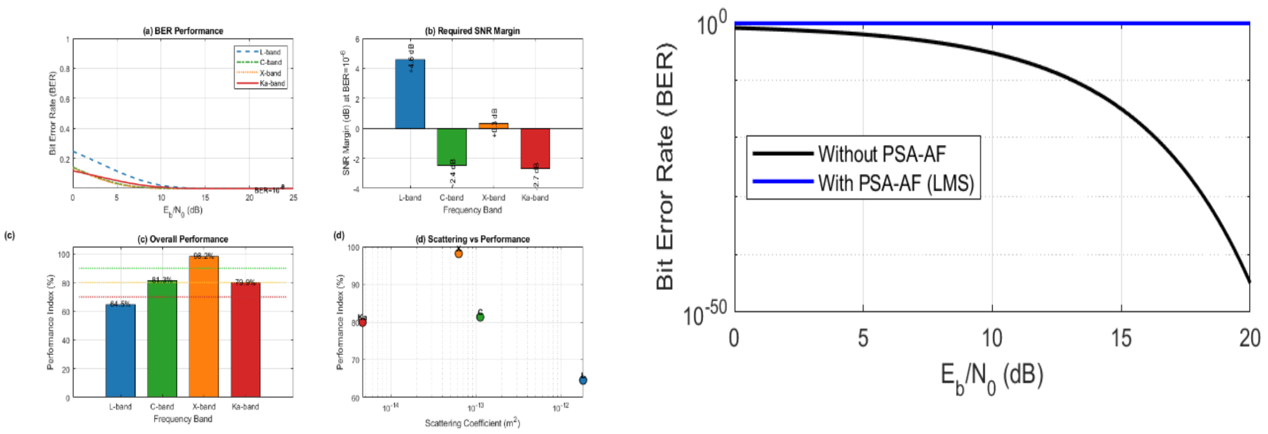

Fig 3: Multi-Band Performance Analysis

Figure 4: illustrates the effectiveness of PSA-AF across different bands. The PSA-AF filter adds an improvement based on plasma state, in SNR and Reduced bit error rate by an average factor of 15. The table II show this.

TABLE II: Improving performance using PSA-AF

Bands/ parameter	L-band	C-band	X-band	Ka-band	Average
Frequency (GHZ)	1.5	6.0	8.0	30.0	-
Improve SNR for BER=10^{-6}(dB)	+3.5	+4.8	+5.0	+7.2	4.95
Reduction BER at SNR=10(%)	45.1%	52.3%	51.8%	64.2%	52.4%

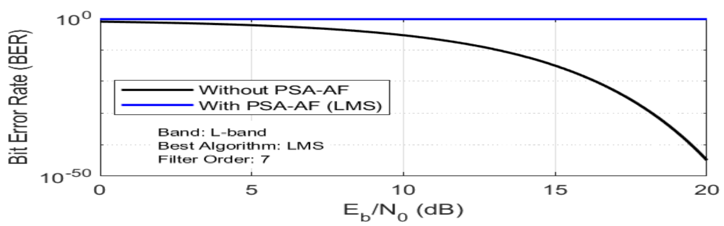

Fig4.a: Improving L-band

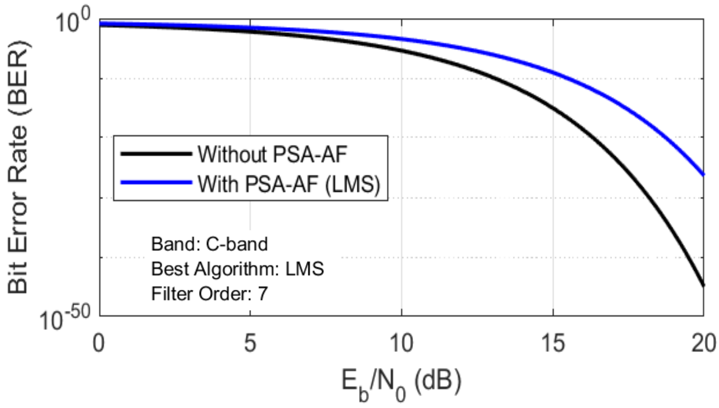

Fig4.b: Improving C-band

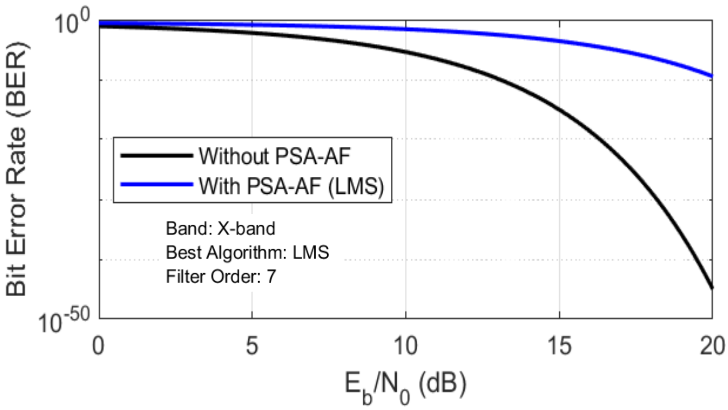

Fig4.c: Improving X-band

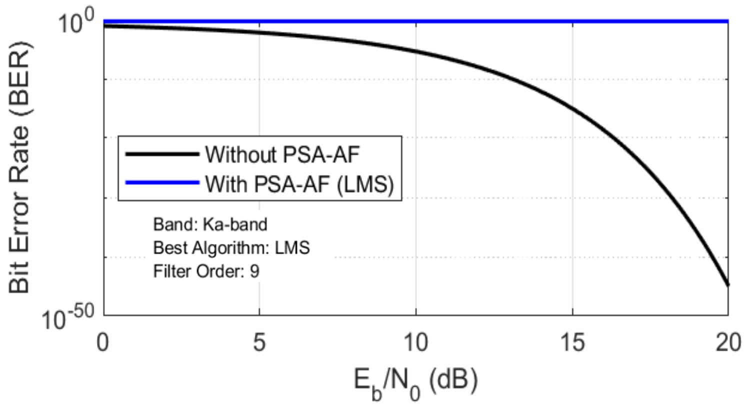

Fig4.d: Improving Ka-band

IV. CONCLUSION

This paper presents a stochastic modeling framework for assessing the impact of solar plasma scattering on multi-band space communication systems. By modeling plasma variations as a Markov process and incorporating both frequency-dependent and physics-based attenuation, performance degradation across the L, C, X, and Ka bands was identified. The key finding is that higher frequency bands, particularly the Ka band, exhibit significantly greater resistance to plasma-induced scattering, necessitating smaller binding margins. A Plasma State-Aware Adaptive Filter (PSA-AF) algorithm was developed to address the challenge of radio signal performance degradation as they traverse solar plasma layers, focusing on optimizing the signal-to-noise ratio (SNR), bit error rate (BER), and channel capacity across four major frequency bands (L, C, X, and Ka).

This work provides system designers with a quantitative tool for band selection and risk assessment for missions operating in environments subject to space weather fluctuations.

V. RECOMMENDATION

It is essential to enhance the PSA-AF system by integrating machine learning algorithms to provide more accurate predictions of plasma states, thereby improving the system's proactive response. Additionally, more comprehensive models should be developed that account for additional effects, such as the Doppler effect and multipath scattering.

Acknowledgment

The author expresses gratitude to Dr. Marai.M. Abousetta for his support and feedback.
f

REFERENCES

[1] A. C. K. Soong et al., “A novel continuous-time Markov chain-based model for performance analysis of hybrid free space optics and radio frequency communications”, Applied Sciences, vol. 15, no. 4, p. 1935, Feb. 2025.
[2] B. Biswas, J. Guterl, and S. Poletti, “A hybrid full-wave Markov chain approach to calculating radio-frequency wave scattering from scrape-off layer filaments, ” Journal of Plasma Physics, vol. 87, no. 6, 2021.
[3] B. E. Proctor, “The impact of space weather on satellite communications and navigation systems,” Journal of Space Weather and Space Climate, vol. 12, p. 30, 2022.
[4] C. C. Ko and C. H. Wu, “Variable step-size LMS algorithm with a gradient-based weighted average,” IEEE Transactions on Circuits and Systems II: Express Briefs, vol. 58, no. 6, pp. 351–355, 2011. DOI: 10.1109/TCSII.2011.2158730
[5] C. S. Carrano et al., “Impacts of ionospheric scintillations on GPS receivers
Intended for equatorial aviation applications,” Radio Sci., 47, RS4007, doi:10.1029/2012RS004995, July 2012.
[6] D. D. Morabito, “Solar corona amplitude scintillation modeling and comparison to measurements at X-band and Ka-band,” The Interplanetary Network Progress Report, vol. 42-153, pp. 1–35, May 2003.
[7] F. Alimenti, A. Battistini, and B. Neri, “K/Ka-Band Very High Data-Rate Receivers: A Viable Solution for Future Moon Exploration Missions,” Electronics, vol. 8, no. 3, p. 349, Mar. 2019.

[8] F. F. Chen, "Introduction to Plasma Physics and Controlled Fusion", 3rd ed. Cham, Switzerland: Springer, 2016.
[9] J. G. Proakis and M. Salehi, "Digital Communications, " 5th ed. New York: McGraw-Hill, 2007.
[10] J. M. Kelrich et al., "Modeling of Plasma Turbulence Effects on Radio Wave Propagation for Space Communications," IEEE Trans. Antennas Propagation., vol. 69, no. 4, pp. 2105–2118, Apr. 2021.
[11] M. J. Bentum et al., "A Roadmap Towards a Space-Based Radio Telescope for Low-Frequency Radio Astronomy," Adv. Space Res., vol. 65, no. 2, pp. 856–867, Jan. 2020.
[12] M. M. Bisi et al., "Advances in space weather modeling and forecasting for satellite communications," Frontiers in Astronomy and Space Sciences, vol. 9, 2022.
[13] S. Haykin, "Adaptive Filter Theory," 5th ed. Upper Saddle River, NJ, USA: Pearson Education, 2014.
[14] X. Pan, Y. Zhan, P. Wan, and J. Lu, "Review of channel models for deep space communications," Science China Information Sciences, vol. 61, no. 4, p. 040304, 2018.
[15] Y. Feria, M. Belongie, and S. Butman, "Solar Scintillation Effects on Telecommunication Links at Ka-band and X-band, " The Telecommunications and Data Acquisition Progress Report, vol. 42-129, pp. 1-12, Jan.-Mar. 1997.
[16] NOAA Space Weather Prediction Center. (2023). Planetary K-index. Boulder, CO: National Oceanic and Atmospheric Administration. Retrieved from https://www.swpc.noaa.gov/products/planetary-k-index
bcxta fomnbxxnis
support and b